Modeling plasma-based CO_2 conversion : crucial role of the dissociation cross section

Reference:

Bogaerts Annemie, Wang Weizong, Berthelot Antonin, Guerra Vasco.- Modeling plasma-based CO_2 conversion : crucial role of the dissociation cross section

Plasma sources science and technology / Institute of Physics - ISSN 0963-0252 - 25:5(2016), 055016

Full text (Publishers DOI): http://dx.doi.org/doi:10.1088/0963-0252/25/5/055016

Modeling plasma-based CO_2 conversion: Crucial role of the dissociation cross section

Annemie Bogaerts[1], Weizong Wang[1], Antonin Berthelot[1] and Vasco Guerra[2]

[1] Research group PLASMANT, Department of Chemistry, University of Antwerp, Universiteitsplein 1, BE-2610 Wilrijk-Antwerp, Belgium. E-mail: annemie.bogaerts@uantwerpen.be

[2] Instituto de Plasmas e Fusão Nuclear, Instituto Superior Técnico, Universidade de Lisboa, 1049-001 Lisboa, Portugal

Abstract

Plasma-based CO_2 conversion is worldwide gaining increasing interest. A large research effort is devoted to improving the energy efficiency. For this purpose, it is very important to understand the underlying mechanisms of the CO_2 conversion. The latter can be obtained by computer modeling, describing in detail the behavior of the various plasma species and all relevant chemical processes. However, the accuracy of the modeling results critically depends on the accuracy of the assumed input data, like cross sections. This is especially true for the cross section of electron impact dissocation, as the latter process is believed to proceed through electron impact excitation, but it is not clear from literature which excitation channels effectively lead to dissocation. Therefore, the present paper discusses the effect of different electron impact dissociation cross sections reported in literature on the calculated CO_2 conversion, for a dielectric barrier discharge (DBD) and a microwave (MW) plasma. Comparison is made to experimental data for the DBD case, to elucidate which cross section might be the most realistic. This comparison reveals that the cross sections proposed by Itikawa and by Polak and Slovetsky both seem to underestimate the CO_2 conversion. The cross sections recommended by Phelps with threshold of 7 eV and 10.5 eV yield a CO_2 conversion only slightly lower than the experimental data, but the sum of both cross sections overestimates the values, indicating that these cross sections represent dissociation, but most probably also include other (pure excitation) channels. Our calculations indicate that the choice of the electron impact dissociation cross section is crucial for the DBD, where this process is the dominant mechanism for CO_2 conversion. In the MW plasma, it is only significant at pressures up to 100 mbar, while it is of minor importance for higher pressures, when dissociation proceeds mainly through collisions of CO_2 with heavy particles.

1. Introduction

CO_2 conversion into value-added chemicals or new fuels by means of plasma technology is gaining increasing interest. Plasma is indeed very promising for energy-efficient CO_2 conversion, because it creates energetic electrons that can activate the gas molecules by electron impact dissociation, ionization and excitation, and the reactive species created in this way (i.e., radicals, ions, excited species) can easily form new products. Thus, the gas does not have to be heated as a whole, and strongly endothermic reactions, like CO_2 splitting and the dry reforming of methane (i.e., simultaneous conversion of $CO_2 + CH_4$), can still occur at mild reaction conditions of temperature and pressure.

Two types of plasma reactors are most commonly used for this purpose: dielectric barrier discharges (DBDs) [1-5] and microwave (MW) plasmas [6-10]. A DBD typically operates at atmospheric pressure and the gas is near room temperature, while the electron temperature is typically several eV. In a MW plasma, the gas is around 500-2000 K, depending on power and pressure, with an electron temperature of about 1 eV. This is most suitable for exciting the vibrational levels of CO_2, which is very important for energy efficient CO_2 splitting [11].

As plasma is created by applying electric power, the energy efficiency of CO_2 conversion is critical for industrial implementation. The highest energy efficiency up to now was reported in 1983 for a MW plasma, i.e., up to 90% [6], but this was at very specific conditions, i.e., supersonic gas flow and reduced pressure (~100-200 Torr), and a pressure rise to atmospheric pressure, which would be desirable for industrial implementation, yields a drop in energy efficiency to 40% [11]. Moreover, this high value of 90% has not yet been reproduced since then. The highest energy efficiency for a MW plasma reported recently was 55% [8], but again for reduced pressure and supersonic flow. Recently, also an energy efficiency of 50% was obtained for a MW plasma at atmospheric pressure, when applying a reverse vortex flow [10]. The energy efficiency of a DBD is more limited, i.e., up to 10% for a conversion of 30% [2], but it can be improved by inserting a (dielectric) packing in a so-called packed bed DBD reactor [3-5]. Moreover, it operates at atmospheric pressure, and has a very simple design, which is beneficial for upscaling, and therefore it also has potential for industrial applications, especially because it can easily be combined with a catalyst, targetting the selective production of value-added chemicals.

To improve the conversion and energy efficiency in these plasma reactors, a better insight in the underlying mechanisms is greatly needed. Computer modeling is very suitable for this purpose, because it allows to unravel the individual processes. In previous years, some models have been developed for CO_2 conversion in a DBD and MW plasma, either in pure CO_2 [2,12-16] or in mixtures with CH_4 [17,18] or N_2 [19,20], while the electron kinetics in CO_2/CH_4 mixtures was analysed in [21]. It was reported that electron impact excitation to the electronically excited states of CO_2, followed by dissociation, is the dominant process for CO_2 conversion in a DBD [12,22], while in a MW plasma, the electrons with lower energy mainly give rise to excitation of the (asymmetric mode) vibrational levels of CO_2, followed by vibration-vibration relaxation collisions, populating the higher vibrational levels, which finally will dissociate, i.e., so-called ladder climbing [11,13,22]. The latter process requires less energy for dissociation than excitation to the electronically excited levels, and this explains the higher energy efficiency of a MW plasma.

In spite of the interesting new insights obtained already by computer modeling, the accuracy of the modeling results strongly depends on the accuracy of the cross sections used. The main cross sections for electron impact reactions with CO_2 are listed in the LXCat database [23], and are mostly collected by Phelps [24,25], although the dissociation cross section is only listed in the Itikawa database of LXCat [26]. Recently, Grofulović et al. have updated this cross section set, by validating it against swarm data (i.e., the reduced Townsend ionization coefficient, the characteristic energy, the longitudinal diffusion coefficient and mobility), and a paper about this work will soon be submitted [27]. There is, however, quite some uncertainty about the cross section for electron impact dissociation through excitation to the electronically excited levels, as is also outlined in [27]. Different authors use or provide cross sections for dissociation which often significantly differ. One difficulty seems to arise from limitations in measuring the possible reaction products.

In the previous works from the PLASMANT team at University of Antwerp, the cross section reported by Itikawa [26] with a threshold of 11.9 eV has always been used [2,12-14,16-20], because it is indeed explicitly mentioned in [26] as “electron impact dissociation”, while the other relevant cross sections in LXCat, with lower thresholds of 7 eV and 10.5 eV, are explictly tabulated as “electron impact excitation”, without referring to dissociation.

Ponduri et al. [15] recently applied a 1D fluid model, based on a very similar plasma chemistry as developed in the PLASMANT group [13,14] to model CO_2 conversion in a DBD. When they assume only electron impact dissociation based on Itikawa’s cross section, their calculated CO_2 conversion was about one order of magnitude lower than experimental values, obtained in a wide range of specific energy input (SEI). In contrast, when they also included the contribution of the electronically excited states with energy at 7 eV and 10.5 eV, corresponding to both excitation processes reported by Phelps, their calculated CO_2

conversion was too high. However, when only including the contribution from the lowest excited level at 7 eV, corresponding to Pietanza's work, a reasonable agreement with experiments was reached, although the calculated CO_2 conversion was still overestimated by a factor 2. The authors concluded that further work is needed to clarify the role of the different reaction channels contributing to CO_2 dissociation.

Pietanza et al. [28-30] advise to use the excitation cross section reported by Phelps, with threshold of 7 eV, as the dissociation channel, while they consider the process with threshold of 10.5 eV as normal electronic excitation. In their recent paper [31], they have performed a parametric evaluation, for a wide range of reduced electric fields and vibrational temperatures, to compare the calculated EEDF and the CO_2 dissociation rates in pure CO_2 plasmas, using two different electron impact excitation-dissociation cross sections, more specifically, the data from Phelps [23-25] with a threshold of 7 eV, and the ones of Cosby and Helm [32], with a threshold of 12 eV. They reported differences up to orders of magnitude, depending on the reduced electric field assumed. The authors also concluded that a more complex theoretical and experimental work on CO_2 dissociation, by means of a full chemical kinetics model, is needed to eliminate the existing large uncertainties in the electron impact dissociation cross sections.

Fridman [11] reports cross section sets representing CO_2 dissociation from two different studies. The first one is based on the theoretical calculations by Polak and Slovetsky [33], assumed in [11] to accurately describe dissociation. These cross sections contain two maxima, with a low and a high threshold energy. The first maximum comes from dissociation by excitation to the states with energy ~7-9 eV through allowed transitions, while the second maximum corresponds to dissociation with the formation of CO(a). A minor contribution from the excitation of the 7-9 eV states through forbidden transitions is also identified, but it is much smaller than the previous two channels and will be disregarded. When considering both excitation processes reported by Phelps, i.e., with thresholds of 7 eV and 10.5 eV, the cross section similarly exhibits two maxima, but the results of Ponduri et al. [15] suggest that these processes may overestimate the CO_2 conversion, so they probably contain more channels than only dissociation. This is indeed not clearly mentioned in Phelps' reports [23-25]. Indeed, as stated in [27], these cross sections seem not to correspond to a specific process, but rather to a combination of excitations to various levels, lumped as global energy loss.

The second cross section reported in [11] was proposed by Corvin and Corrigan [34], with threshold at 6.1 eV. However, this cross section is estimated by trying to reproduce a measured dissociation rate using a Maxwellian electron energy distribution function (EEDF). We believe that this approach is less suitable and this cross section will not be considered in this work.

The total dissociation cross section from Polak and Slovetski [33] differs significantly from the cross section provided by Corvin and Corrigan [34], both in shape and magnitude (see figure 7 of ref. [27]). However, it is more or less similar in shape to the electronic excitation cross sections with thresholds of 7 eV and 10.5 eV, reported by Phelps, but somewhat shifted in energy values and also much smaller in magnitude (see again figure 7 of [27], and also section 2.2 below). This again suggests that the excitation cross sections reported by Phelps probably include more channels than pure dissociation.

In their recent paper [27], Grofulović et al. indeed mention that the cross sections reported by Phelps do not correspond to any specific process, but rather to a combination of mechanisms lumped as a global energy loss. They most likely do represent dissociative channels, but they may also contain more than just dissociation. Furthermore, the authors suggest that the cross sections of Polak and Slovetsky might provide a realistic picture of electron impact dissociation of CO_2, but they state that further investigations on the effect of the different cross section sets on the CO_2 dissociation are highly desirable.

Therefore, in the present paper, we will evaluate the effect of the different dissociation cross sections on the CO_2 conversion in real plasma conditions. More specifically, based on the arguments provided above,

we will compare the cross section reported by Itikawa [26] (which probably underestimates the dissociation), Phelps [23-25] and Polak and Slovetsky [33]. A plot of these cross sections as a function of electron energy, as well as the corresponding rate coefficients of these processes as a function of both electron energy and reduced electric field, will be illustrated in section 2.2 below.
This study will be performed by a 0D model, which is most suitable to include the detailed plasma chemistry, needed to assess this effect. The model will be applied to a DBD and MW plasma. In a DBD, this process should be the dominant dissociation mechanism, so we expect a significant difference in the results, especially for the cross section proposed by Itikawa, due to its high threshold energy of 11.9 eV. Indeed, the cross sections of Phelps and of Polak and Slovetsky allow all electrons with energy between 7 and 11.9 eV to contribute to dissociation of CO_2, while this is not possible with Itikawa's cross section. By comparison with experimental values for the CO_2 conversion as a function of SEI, we aim to provide some insight into which cross section should be the most accurate. In a MW plasma, we expect this process to be of lower importance, as revealed by our previous modeling studies [13,14]. However, these studies were performed with the cross section adopted from Itikawa, and a cross section with lower energy threshold might indicate that this process is not negligible. Therefore, it is also very interesting to compare the calculations for the different cross sections at MW conditions.

In section 2, we will give a brief explanation about the 0D model, the cross sections used and the assumptions made for the DBD and MW plasma reactors. The results for both cases will be presented and discussed in section 3, and finally the conclusions will be given in section 4.

2. Description of the model, the cross sections and the plasma reactor assumptions

2.1. Description of the model

The model used to calculate the CO_2 conversion is a 0D chemical kinetics model, called ZDPlaskin, developed by Panchesniy [35]. It solves balance equations for the various plasma species (see below), based on production and loss rates, as defined by the chemical reactions in the plasma:

$$\frac{dn_i}{dt} = \sum_j \left\{ \left(a_{ij}^{(2)} - a_{ij}^{(1)} \right) k_j \prod_l n_l^{a_{lj}^{(1)}} \right\}$$

In this equation, $a_{ij}^{(1)}$ and $a_{ij}^{(2)}$ are the stoichiometric coefficients of species i, at the left and right hand side of a reaction j, respectively, n_l is the species density at the left hand side of the reaction, and k_j is the rate coefficient of reaction j. The species included in the model are listed in Table 1.

Table 1: Overview of the species included in the CO_2 model.

Molecules	Charged species	Radicals	Excited species
CO_2, CO	CO_2^+, CO_4^+, CO^+, $C_2O_2^+$, $C_2O_3^+$, $C_2O_4^+$, C_2^+, C^+, CO_3^-, CO_4^-	C_2O, C, C_2	CO_2(Va, Vb, Vc, Vd), CO_2(V1-V21), CO_2(E1, E2), CO(V1-V10), CO(E1-E4)
O_2, O_3,	O^+, O_2^+, O_4^+, O^-, O_2^-, O_3^-, O_4^-	O	O_2(V1-V4), O_2(E1-E2)
	electrons		

The symbols "V" and "E" between brackets for CO_2, CO and O_2 represent the vibrationally and electronically excited levels of these species, respectively. Details about these notations can be found

in [13,14]. We describe in detail the asymmetric stretching mode of vibrational excitation for CO_2, because it provides the most important channel for dissociation [11], so we take into account all the CO_2 asymmetric mode levels up to the dissociation energy of 5.5 eV (i.e., 21 levels, denoted by numbers (V1-V21) in Table 1 above), while only 4 effective low-lying symmetric stretching and bending mode levels are included for CO_2 in the model (denoted by Latin letters (Va-Vd) in Table 1). Furthermore, we take into account two electronically excited states of CO_2 (indicated as E1 and E2), but depending on the dissociation cross section assumed in the model, one of them, or even both of them, will be considered as dissociative channel (see section 2.2 below).

A large number of chemical reactions is incorporated in this model, including various electron impact reactions, electron-ion recombination reactions, ion-ion, ion-neutral and neutral-neutral reactions, as well as vibration-translation (VT) and vibration-vibration (VV) relaxation reactions, and the effect of vibrational excitation on the other chemical reactions. All details about these chemical reactions, and the corresponding rate coefficients and/or theories behind it in order to estimate these values, can be found in [13].

Stepwise electron impact excitation of the vibrational levels from v=0,1,2,3,4,5 and a,b,c,d to all the other asymmetric mode vibrational levels, as well as stepwise electron impact excitation from the vibrational levels to the electronically excited levels, and (stepwise) electron impact ionization from the various vibrational levels, are included in the model, but stepwise excitation of the electronically excited levels is not taken into account, because only two, and sometimes even one (or no) electronically excited level, depending on the cross section used for electron impact dissociation (as explained above), is considered in the model (see Table 1). It seems that there is not much data available in literature on the electronic states of CO_2 (see also the Introduction)."

Note that CO and O_2 are the main products of the CO_2 dissociation. Their reactions, including the recombination to form again CO_2, are also included in the model. This is one of the explanations why the CO_2 conversion does not rise linearly upon increasing residence time or specific energy input, but starts to level off, as shown for instance in one of our previous papers [2]. Moreover, our model predicts that in a MW plasma, the conversion and energy efficiency, although typically higher than in a DBD, are further limited by the recombination of O atoms (formed upon CO_2 splitting) into O_2 molecules. If the O atoms can be used for further dissociation of CO_2, through the reaction $CO_2 + O \rightarrow CO + O_2$, instead of recombining into O_2 molecules, the CO_2 conversion and energy efficiency in the MW plasma could be further enhanced. One possibility might be to trap part of the O atoms, so that the recombination probability into O_2 molecules could be reduced, but this certainly needs further investigation in the future.

The balance equations yield the time-evolution of the species densities. The 0D model does not account for transport processes in the plasma, and no surface reactions are taken into account, but spatial variations in the plasma reactor, e.g., due to the power deposition or gas temperature, can be accounted for by translating the spatial evolution into a time evolution by means of the gas flow rate. Indeed, when the gas molecules pass through the plasma reactor, they experience spatial effects from the power deposition and the gas temperature, which can be accounted for by temporal effects, as will be explained below for both the DBD and MW plasma. Hence, the plasma reactors are considered as plug flow reactors, where the concentration of the gas changes as a function of distance travelled through the reactor, or as a function of residence time, in a similar way as would be the case for the temporal evolution in a batch reactor, thus motivating the use of a 0D model. Besides, due to the large chemistry that needs to be included to accurately predict the CO_2 conversion, a 0D model is the most suitable approach, because a model in more dimensions would yield much longer calculation times.

Besides the species densities, also the average electron energy is calculated in this model, based on an energy balance equation, again with energy source and loss terms as defined by the chemical reactions. The average electron energy is used to calculate the energy-dependent rate coefficients of the electron-induced processes, such as ionization, excitation and dissociation, from the EEDF and the corresponding cross sections (see below). The rate coefficients of the other chemical reactions, i.e., between the neutral species or ions, depend on the gas temperature and are calculated from Arrhenius equations, using data adopted from literature (see [13] for the details).

The energy efficiency (η) is calculated in our model with the following formula:

$$\eta(\%) = \frac{\Delta H_R \left(\frac{kJ}{mol}\right) * X_{CO_2}(\%)}{SEI\left(\frac{kJ}{l}\right) * 22.4\left(\frac{l}{mol}\right)}$$

where ΔH_R is the reaction enthalpy for CO_2 splitting (i.e., 279.8 kJ/mol), X_{CO_2} is the CO_2 conversion and SEI is the specific energy input, which is defined from the power introduced in the plasma and the gas flow rate:

$$SEI\left(\frac{kJ}{l}\right) = \frac{Plasma\ power\ (kW)}{Flow\ rate\ (\frac{l}{min})} * 60\left(\frac{s}{min}\right)$$

Note that the CO_2 conversion and energy efficiency typically show the opposite behavior as a function of SEI, i.e., a high SEI yields a higher CO_2 conversion, but the energy efficiency is more limited and vice versa. The reason can be understood from the above formula: the energy efficiency is proportional with the CO_2 conversion, but inversely proportional with the SEI. When the CO_2 conversion does not rise to the same extent as the SEI, the energy efficiency will drop upon rising energy efficiency, as demonstrated for instance in [2,22].

2.2. Description of the cross sections used

The set of electron impact cross sections used in this work to calculate the EEDF was recently proposed by Grofulović et al. [27], and the cross sections are plotted in Figure 1 as a function of electron energy. This set includes the cross sections for effective momentum transfer (MT), vibrational excitation for processes with energy thresholds at 0.083, 0.167, 0.252, 0.291, 0.339, 0.422, 0.505 and 2.5 eV (see [27] for details), dissociative attachment, two electronic excitations (with thresholds of 7 and 10.5 eV), and total ionization. This cross section set is updated from the set proposed by Phelps, which is included in the LXCat database [23], and details about the modifications of this cross section set are given in [27].

In our model, some more electron impact collisions are included, e.g., for vibrational exitation of all vibrational levels within the asymmetric mode (see [13] for details). However, only a limited number of these individual cross sections is available in the set proposed by Grofulović et al. [27], as the remaining transitions are lumped in generic energy losses. Due to the importance of these processes in vibration-induced dissociation of CO_2, they are still included in our model, and the rate coefficients are calculated by integrating the cross sections over the EEDF calculated as explained above. Indeed, it is important to stress that the EEDF is calculated with a consistent set of cross sections that is validated against swarm data.

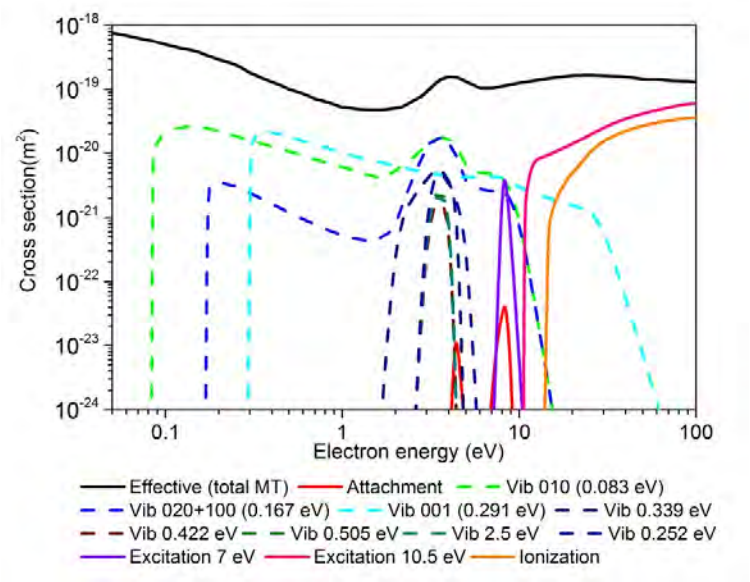

Figure 1: Cross sections of the various electron collisions with CO_2 as a function of electron energy, used in the model to calculate a realistic electron energy distribution function with a two-term Boltzmann solver. This cross section set is proposed by Grofulović et al. [27], to yield a valid prediction of the swarm parameters. More details can be found in [27].

Using the EEDF calculated with the cross sections proposed by Grofulović et al. [27], we tested the effect of different dissociation cross sections, namely:

1) The cross section reported by Itikawa with threshold of 11.9 eV, like it was explicitly mentioned in the LXCat database [23], and which we had thus adopted in our previous studies [2,12-14,16-20]. In this case, the processes with thresholds as 7 eV and 10.5 eV, as adopted from Phelps, are considered as purely electronic excitation.
2) The cross sections reported by Phelps [23-25], with the 7 eV threshold considered as dissociation, and the 10.5 eV threshold as electronic excitation. In this case, we have only 1 CO_2 electronically excited state in the model (cf. Table 1 above). This approach is also used by Pietanza et al. [28-30].
3) The cross sections reported by Phelps [23-25], with the 7 eV threshold considered as electronic excitation, and the 10.5 eV threshold as dissociation (hence the opposite of case 2, with again only 1 CO_2 electronically excited state in the model);
4) The cross sections reported by Phelps [23-25], with both the 7 eV and 10.5 eV thresholds considered as dissociation;
5) The cross sections calculated by Polak and Slovetsky [33], accounting for two channels of dissociation.

For the sake of comparison, these various "dissociation" cross sections, i.e., the data suggested by Itikawa, both cross sections reported by Phelps, with thresholds of 7 eV and 10.5 eV, and the total cross section calculated by Polak and Slovetsky (from here on simply called "Polak"), are plotted as a function of electron energy in Figure 2. It is clear that the Itikawa cross section not only has a much higher threshold, but also lower absolute values. Furthermore, the Polak cross section is also clearly lower than both Phelps cross sections. Especially the Phelps cross section with threshold of 10.5 eV reaches high values, but typically at electron energies above 15 eV, which is not common in the plasma types under study.

The corresponding dissociation rate coefficients, as calculated from the cross sections and the EEDF, are plotted in Figure 3, both as a function of electron energy and reduced electric field. Note that the typical electron energy calculated in our DBD model is around 5 eV (see section 3.1 below), while in the MW model, the electron energy is calculated to be 1-2 eV (see section 2.4 below).

At low values of electron energy (~ 1-2 eV) and low values of reduced electric field (~ up to 100 Td), the Phelps cross section with threshold of 7 eV yields the highest dissociation rate coefficient, but at higher electron energies and reduced electric fields, the Phelps cross section with 10.5 eV threshold dominates, and the Phelps cross section with 7 eV threshold yields a rate coefficient that is comparable to the values calculated with the Polak cross section. The rate coefficient as calculated by Itikawa's cross section is always at least one order of magnitude lower than the rate coefficients calculated by the other cross sections. For comparison, Figure 3 also illustrates the ionization rate coefficient (dashed line). It is comparable to the dissociation rate coefficient calculated with Itikawa's cross section at low electron energies and reduced electric fields, but rises more rapidly for electron energies above 2-3 eV, or reduced electric fields above 150 Td, and at electron energies above 6 eV and reduced electric fields above 400 Td, it becomes even comparable to the dissociation rate coefficients calculated with Polak's cross section and the Phelps cross section with threshold of 7 eV. This is important to keep in mind, as ionization can also lead to dissociation (after dissociative electron-ion recombination of the formed CO_2^+ ion); see the results section below.

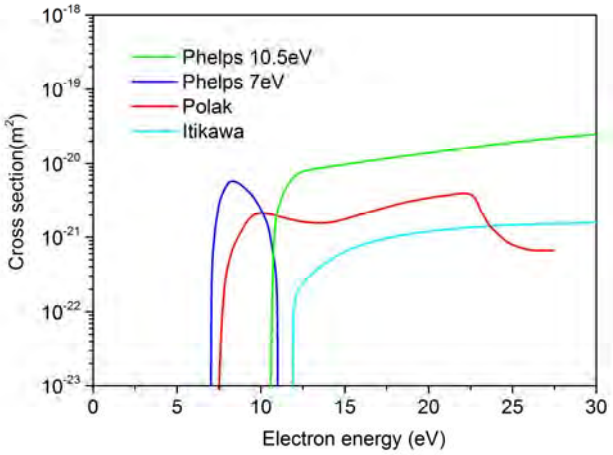

<u>Figure 2:</u> Comparison between the different cross sections for electron impact excitation-dissociation of the CO_2 ground state, used in our study, as a function of electron energy.

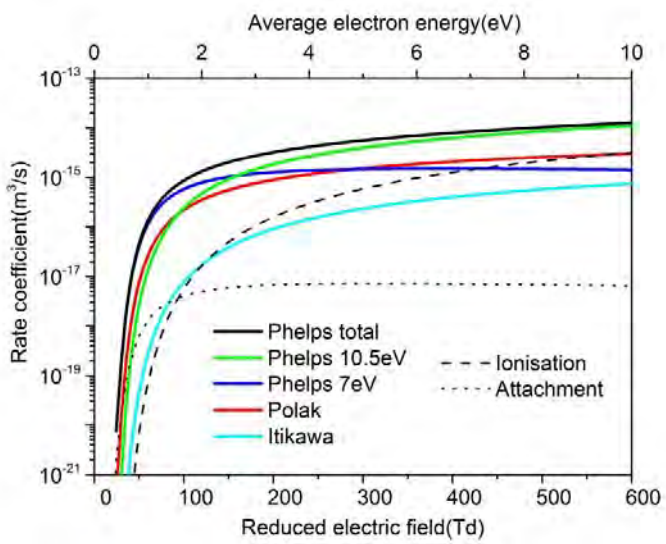

Figure 3: Comparison between the dissociation rate coefficients, calculated with the different cross sections, as a function of average electron energy and reduced electric field. For comparison, the rate coefficients for ionization and dissociative attachment are also plotted (with dashed and dotted line, respectively).

2.3. Description of the DBD plasma with the 0D model

The DBD plasma reactor under study is a cylindrical plug flow reactor, consisting of a central grounded copper electrode, with diameter of 22 mm, surrounded by a coaxial alumina tube, with inner and outer diameter of 26 and 30 mm, respectively. This tube is covered by a stainless steel mesh, which serves as the outer electrode and is powered by a high voltage source. The length of the outer electrode is 10 cm, and this defines the length of the plasma zone. Hence, the plasma reactor volume is 15.08 cm^3. More details about this setup can be found in [36]. We applied our model to this specific reactor geometry, as it was used to measure some filament properties, which we need in our model (see below).

A DBD plasma in CO_2 operates in filamentary mode. Hence, the CO_2 gas molecules will pass through filaments when travelling through the plasma reactor. Although the model is 0D, this filamentary character can be taken into account by applying current pulses as a function of time, mimicking the filaments as a function of space (cf. section 2.1 above). The electron impact processes and chemical reactions occurring during these filaments, as well as in the time between the filaments, i.e., the so-called afterglows, are described in detail in the model (see detailed discussion in [12] for a CO_2 plasma, as well as in [17] for a CO_2/CH_4 plasma). The crucial aspect in modeling CO_2 conversion in a DBD reactor is thus to know the number of filaments that the CO_2 molecules can pass when travelling through the reactor. Indeed, although there exist several filaments per half cycle, they are limited in volume, so not all molecules will pass through all these filaments. In our previous studies, we assumed a certain "filament frequency" in combination with a certain "filament volume", based on common sense, which yielded a CO_2 conversion in reasonable agreement with typical experimental values [1,13,17-19].

In the present paper, we want to evaluate which dissociation cross section yields the most realistic CO_2 conversion, and thus, the exact assumptions of filament frequency and volume (or combined into a so-called "volume-corrected filament frequency"), as well as filament lifetime, are more critical. The problem is that these parameters are not exactly known. We want to make sure that we do not draw false

conclusions, by making wrong assumptions on the filament properties. For that reason, we performed several simulations (each time comparing the different dissociation cross sections), to evaluate the effect of these assumptions.

As stated above, we consider the experimental conditions of [36], because it provides data on the filament lifetime and the number of filaments per half cycle. Indeed, in these experiments, about 200 filaments per half cycle were counted and the average lifetime of the filaments was determined to be 15.6 ns, at a discharge frequency of 28.6 kHz, a gas flow rate of 200 mL/min, and a discharge power of 55W. Moreover, the reactor gas temperature was reported to be ~560 K. The only remaining uncertainty now is the filament size (or filament diameter).

Measuring the filament diameter seems to be non-trivial, as the filaments appear randomly at a time-scale of ~ 10 ns, and they have quite limited dimensions. It is reported that the filament shape drastically depends on the electrode conductivity, e.g., one can observe discharge expansion on the anode surface (i.e., surface discharge) in the so-called M-D+ (i.e., metal negative – dielectric positive polarity) configuration, while mostly a cylindrical shape is reported for the M+D- case [37]. Typical diameters are listed in the range of 0.2 – 0.5 mm in an O_2 plasma with discharge gap of 3 mm, and 0.1 – 0.3 mm in an air plasma in the cathode vicinity (see [37] and references therein). Also in [38,39] typical filament diameters in the order of 0.1 mm are reported. Therefore, we performed simulations for filament diameters of 0.07, 0.1, 0.2, 0.3 and 0.4 mm.

A filament diameter of 0.1 mm in a gap size of 2 mm corresponds to a filament volume of 0.016 mm^3. Comparing this with the plasma reactor volume of 15.08 cm^3 (see above) yields a filament volume fraction of 1.04×10^{-6}. Combining this with the measured number of filaments per half cycle (see above), this gives a so-called "volume-corrected filament frequency" of 2.08×10^{-4} per half cycle, or vice versa "1 filament every 4800 half cycles". In the same way, the filament frequency is calculated for the other filament diameters. Moreover, we also performed calculations for different filament lifetimes, to assess their effect on the CO_2 conversion. In practice, we consider a lifetime of 15.6 ns (as measured in the experiments; see above), as well as 30 ns and 60 ns.

The other input parameters in the model, i.e., plasma power and gas flow rate (which determine the SEI and the gas residence time) and the gas temperature, are taken from the experiments [36] and are mentioned above. With these input data, the calculations run self-consistently and provide the CO_2 conversion and the relative importance of the various processes, for the different dissociation cross sections investigated, as well as the electron density and temperature as a function of time (both during and in between the pulses which characterize the filaments). However, as our earlier calculations revealed that the electron number density can be quite critical in determining the CO_2 conversion [17], we performed a set of calculations with self-consistently calculated electron density (reaching maximum values around 10^{15} cm^{-3}), as well as a set of calculations where we limited the maximum electron density to 10^{14} cm^{-3}, to evaluate this effect on the calculation results as well. Thus in total we performed 70 different calculations for assessing the effect of the assumed parameters, i.e., for 5 different filament diameters (keeping the filament lifetime fixed at 15.6 ns) and 3 different filament lifetimes (keeping the filament diameter fixed at 0.1 mm), each time for self-consistently calculated electron densities and fixed maximum electron densities, and for the 5 different dissociation cross sections investigated. In addition, we performed another set of 20 calculations, for a fixed filament diameter and lifetime, and for the self-consistently calculated electron density, varying the plasma power (and thus the SEI values) for the 5 different cross sections, to compare with the experimental data.

2.4. Description of the MW plasma with the 0D model

The MW plasma reactor considered in this study is a simple surfatron plasma, as presented in Silva et al. [7]. It consists of a quartz discharge tube with inner diameter of 14 mm and length of 25 cm, and a waveguide near the middle of the tube, bringing the microwaves perpendicular to the tube, and thus forming a plasma. Thus, similar to the DBD reactor, we can also consider the MW plasma as a plug flow reactor, assuming a certain MW power deposition profile at the position of the waveguide. This is schematically illustrated in Figure 4(a,b). Hence, the molecules will experience this power deposition profile when traveling through the MW plasma reactor. The exact length of the plasma created by this power deposition profile is not known, but it is kept fixed here at 5 cm, based on [16]. We performed calculations in a wide pressure range. We expect that in reality the plasma length will drop with increasing pressure, so to assess the effect of the assumption of a fixed plasma length, we have also performed calculations with a plasma length of 10 cm at 20 mbar and with a plasma length of 1 cm at 1 bar. The results indicate that, although the CO_2 conversion is somewhat affected by the choice of the plasma length, the observed trends remain the same.

The power deposition illustrated in Figure 4(b) will yield a rise in gas temperature. The latter can be self-consistently calculated in our 0D model, as explained in [16], but for the present purpose of testing the effect of different CO_2 dissociation cross sections, we just assumed a certain gas temperature profile, adopted from [16]. The latter is illustrated in Figure 4(c). The other operating conditions used as input in the model are a gas flow rate of 12 slmin and a plasma power of 1000 W, yielding a SEI of 1.17 eV/molec, which is indeed a typical value for a MW plasma reactor. Furthermore, the gas pressure is varied in the range between 20 mbar and 1 bar (see below). These conditions yield reduced electric field values in the order of 130 Td at atmospheric pressure and 200 Td at 20 mbar, while the electron density and average electron energy are calculated to be around 10^{12} cm^{-3} - 10^{13} cm^{-3} and 1-2 eV, respectively, depending on the pressure, which are also typical values for a MW plasma.

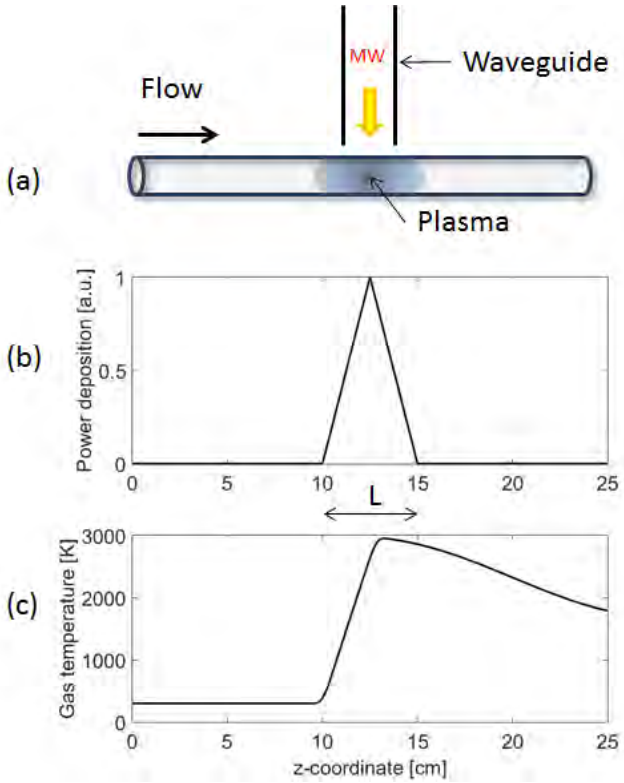

Figure 4: Schematic illustration of the MW plasma reactor geometry (a), shape of the power deposition profile (b) and typical gas temperature profile (c). L denotes the assumed plasma length.

As indicated in our previous work, the CO_2 conversion in a MW plasma is mainly attributed to vibrational excitation of the lowest levels of the asymmetric stretching mode, followed by vibration-vibration relaxation collisions, gradually populating the higher vibrational levels, and finally leading to dissociation, i.e., so-called ladder-climbing, which explains the higher energy efficiency typically found in a MW plasma. Electron impact electronic excitation followed by dissociation was found to be negligible in our model calculations for a MW plasma. However, this was predicted based on Itikawa's cross section, and the higher dissocation cross sections of Phelps and Polak, with lower threshold energies, might yield a larger contribution of this process. Therefore, we also want to investigate the effect of the different CO_2 dissociation cross sections on the CO_2 conversion in a MW plasma, and on the relative importance of the electronic excitation-dissociation pathway. Furthermore, we also observed before that the mechanisms of CO_2 dissociation vary for different pressures [16]. Therefore, as mentioned above, we performed calculations for different pressures, ranging between 20 mbar and 1 bar.

3. Results and discussion

3.1. DBD plasma

First we compare the effect of our assumed values for the filament diameter and filament lifetime, as well as for the electron density, on the calculated CO_2 conversion for the different cross sections, and we try to explain the trends based on the typical filament conditions (like reduced electric field and electron temperature), and on the relative importance of the most important dissociation mechanisms. This comparison will give us a better insight in the validity of the assumptions made. Subsequently, we will calculate the CO_2 conversion as a function of plasma power (and thus SEI value), with a fixed filament diameter and lifetime, for the different dissociation cross sections, and compare the calculation results with experimental data, to provide information on which dissociation cross section gives the most realistic results.

Figure 5 illustrates the calculated CO_2 conversion with the different cross sections outlined in section 2.2 above, as a function of filament diameter, for the maximum electron density ($N_{e,max}$) fixed at 10^{14} cm^{-3} (a), as well as for the self-consistenly calculated electron density, yielding $N_{e,max}$ values typically up to 10^{15} cm^{-3} (b). For simplicity, we call this from now on $N_{e,max} = 10^{15}$ cm^{-3}, but the actual maximum values can be found in Table 2 below. It is clear that the CO_2 conversion calculated with Phelps' total cross section (i.e., sum of the 7 eV and 10.5 eV thresholds) is always the highest, for both $N_{e,max}$ values and all filament diameters investigated. For $N_{e,max} = 10^{14}$ cm^{-3} (Figure 5(a)), Phelps' cross section with threshold of 10.5 eV also yields a high CO_2 conversion, at least for small filament diameters, while for $N_{e,max} = 10^{15}$ cm^{-3} (Figure 5(b)), the CO_2 conversion calculated with this cross section is somewhat lower, and is comparable to the CO_2 conversion calculated with the Phelps 7 eV threshold cross section. The CO_2 conversion calculated with Polak's cross section and especially with Itikawa's cross section is (nearly) always lower. The Itikawa cross section even yields a negligible CO_2 conversion (i.e., order of 0.5%) for $N_{e,max} = 10^{15}$ cm^{-3}, while for $N_{e,max} = 10^{14}$ cm^{-3} the calculated CO_2 conversion is non-negligible, with values up to 6% for the smallest filament diameters investigated.

In general, we can conclude from Figure 5 that the assumed filament diameter has no major influence on the calculated CO_2 conversion for $N_{e,max} = 10^{15}$ cm^{-3}, with only slightly decreasing values upon larger filament diameters. Only for the smallest filament diameters of 0.07 and 0.1 mm, the difference is somewhat larger for the total Phelps cross section, and the reason of this will be explained below. For $N_{e,max} = 10^{14}$ cm^{-3}, on the other hand, the filament diameter has clearly a larger effect, especially for the Phelps 10.5 eV and 7 eV cross sections and for Itikawa's cross section. Indeed, Itikawa's cross section and

the Phelps 10.5 eV cross section yield a higher CO_2 conversion at the smaller filament diameters, while the Phelps 7 eV cross section yields lower values. Again, the reason of this will be explained below.

The measured CO_2 conversion at this condition (i.e., plasma power of 55 W, corresponding to a SEI of 4.2 eV/molec for a gas flow rate of 200 mL/min, as obtained from [36]) is 17.5 %, as indicated with the horizontal dashed line in Figure 5. It is clear that all the individual dissociation cross sections yield a lower CO_2 conversion than the experimental value, in the entire range of filament diameters (except for the Phelps 10.5 eV cross section at the two smallest filament diameters and $N_{e,max} = 10^{14}$ cm^{-3}). On the other hand, the sum of both Phelps cross sections yields a higher CO_2 conversion than the experimental value in almost the entire range of filament diameters (except for the largest filament diameters investigated). Below, we will compare the CO_2 conversions, calculated with the different cross sections, in a wider range of plasma powers (or SEI values), to further assess which cross section yields a realistic CO_2 conversion.

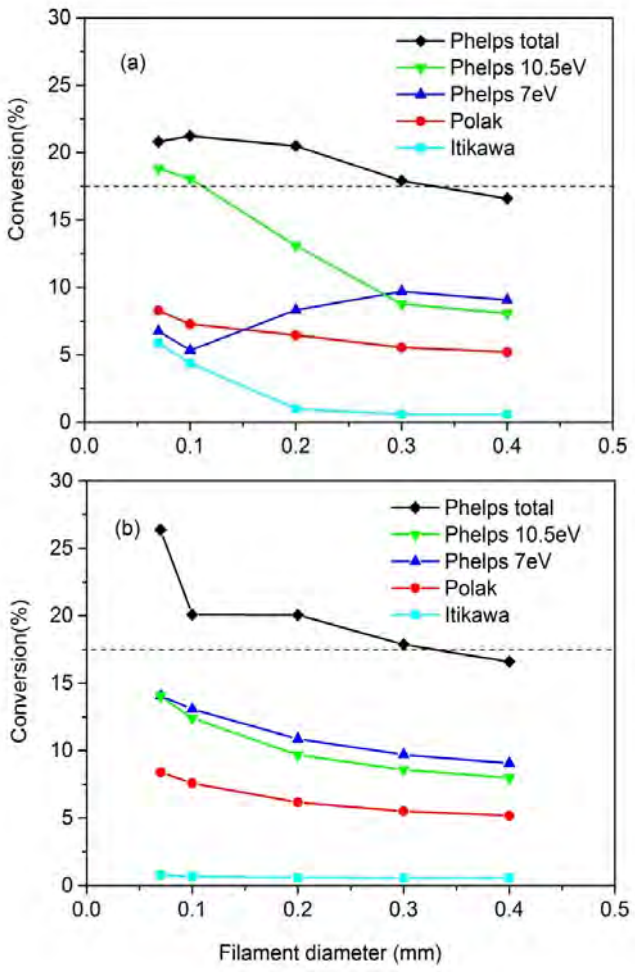

Figure 5: CO_2 conversion in the DBD plasma, calculated with the different dissociation cross sections, as a function of the filament diameter, for $N_{e,max} = 10^{14}$ cm^{-3} (a), and the self-consistently calculated electron density, typically yielding $N_{e,max} \leq 10^{15}$ cm^{-3} (b), for a plasma power of 55 W (or an SEI of 4.2 eV/molec). For comparison, the measured value at this condition, obtained from [36], is indicated with the horizontal dashed line.

The reason why a smaller filament diameter typically yields a somewhat larger conversion, especially for $N_{e,max} = 10^{14}$ cm^{-3}, can be deduced from Table 2, which shows the reduced electric fields (E/N) and average

electron energy inside the filaments, for the different filament diameters and for both $N_{e,max} = 10^{14}$ cm^{-3} and $N_{e,max} = 10^{15}$ cm^{-3}. It is clear that a smaller filament diameter yields a higher reduced electric field, and thus also a higher average electron energy inside the filaments, because it corresponds to a smaller "volume-corrected filament frequency" (see section 2.3 above), so the plasma power is distributed over less filaments, yielding a higher power per filament. The peak power density for the different filament diameters is also listed in Table 2. The effect is most pronounced for $N_{e,max} = 10^{14}$ cm^{-3}, because the available plasma power is distributed over less electrons, yielding a higher average electron energy and also a higher reduced electric field. Indeed, the electric field is obtained as the square root of power divided by electrical conductivity, and the latter is a function of the electron number density. For the largest filament diameter investigated (0.4 mm), there is no difference between $N_{e,max} = 10^{14}$ cm^{-3} and $N_{e,max} = 10^{15}$ cm^{-3}, because the self-consistently calculated electron density is lower than 10^{14} cm^{-3} (cf. the actual N_e values for the different filament diameters, which are also indicated in Table 2).

On the other hand, as the smaller filament diameter corresponds to a smaller "volume-corrected filament frequency" (see above), this entails a lower number of filaments over the entire gas residence time, and thus a shorter "plasma processing time", as is also obvious from Table 2. The latter is of course independent from the maximum electron density considered in the model. These two effects, i.e., the higher reduced electric field and correspondingly higher average electron energy inside the filaments on one hand, and the smaller plasma processing time on the other hand, thus have opposite influence on the calculated CO_2 conversion. In general, the higher reduced electric field and average electron energy inside the filaments have more impact, and they yield a higher CO_2 conversion, because of the higher dissociation rate coefficient, plotted in Figure 3 above. This is most apparent for the Phelps 10.5 eV and Itikawa cross sections, which have a higher threshold, so their rate coefficient rises more upon higher reduced electric field and average electron energy (see Figure 3). The Phelps 7 eV cross section shows the opposite trend, because due to its lower threshold, the dissociation rate coefficient does not rise upon higher reduced electric field or average electron energy (see Figure 3), and the other effect, i.e., a smaller plasma processing time, now dominates, explaining why the CO_2 conversion is lower for the smaller filament sizes, as appears from Figure 5(a).

Table 2: Calculated values of the reduced electric field (E/N), peak average electron energy, and actual values of the electron number density within the filaments, for the different filament diameters and $N_{e,max} = 10^{14}$ cm^{-3} and 10^{15} cm^{-3}. The peak power density within the filament and the total plasma processing time for the sum of all filaments, given the fixed gas residence, are also indicated.

Filament diameter (mm)	E/N(Td)		Average electron energy(eV)		Electron density (cm^{-3})		Peak power density P_d(W/cm^3)	Plasma processing time(μs)
	$N_{e,max}$= 10^{14} cm^{-3}	$N_{e,max}$= 10^{15} cm^{-3}	$(N_e)_{max}$= 10^{14} cm^{-3}	$(N_e)_{max}$= 10^{15} cm^{-3}	$(N_e)_{max}$= 10^{14} cm^{-3}	$(N_e)_{max}$= 10^{15} cm^{-3}		
0.07	920.22	210.0	12.60	5.72	10^{14}	1.63x 10^{15}	7.92x10^7	0.22
0.10	684.27	195.59	10.70	5.49	10^{14}	8.99x10^{14}	3.99x10^7	0.44
0.20	320.29	177.59	7.20	5.20	10^{14}	2.59x10^{14}	9.78x10^6	1.77
0.30	193.32	172.48	5.46	5.11	10^{14}	1.20x10^{14}	4.28x10^6	3.98
0.40	171.02	171.02	5.08	5.08	6.83x10^{13}	6.83x10^{13}	2.42x10^6	7.08

To better understand how the calculated CO_2 conversion varies with the filament diameter and with the dissociation cross section used, at $N_{e,max} = 10^{14}$ cm^{-3} and $N_{e,max} = 10^{15}$ cm^{-3}, we plot in Figure 6 the relative contributions of the various dissociation mechanisms as a function of the filament diameter, for both

$N_{e,max}$ = 10^{14} cm^{-3} and $N_{e,max}$ = 10^{15} cm^{-3}. In general, electron impact dissociation (through electronic excitation, i.e., the process for which the cross sections are evaluated here) is the most important conversion mechanism. This is especially true at $N_{e,max}$ = 10^{15} cm^{-3} (Figure 6(b)), where this process is clearly dominant for all filament diameters investigated, and all dissociation cross sections, except Itikawa's cross section. Indeed, the latter yields a relative contribution of only about 40% for electron impact dissociation, for all filament diameters, which is of course attributed to its smaller cross section, while electron impact ionization (forming CO_2^+ ions, which subsequently dissociate by electron-ion recombination) also contributes for about 40%, and electron impact dissociative attachment contributes for about 10%.

At $N_{e,max}$ = 10^{14} cm^{-3}, electron impact dissociation is also the dominant conversion mechanism for all cross sections except Itikawa's cross section, but its relative importance clearly drops for the smaller filament diameters, especially for the Phelps 7 eV and Polak cross sections, while electron impact ionization becomes increasing important for the smaller filament diameters, and its contribution to the CO_2 conversion becomes even comparable to the contribution of electron impact dissociation for the Phelps 7 eV and Polak cross sections. The situation is even more extreme for Itikawa's cross section, where electron impact ionization is obviously the most important conversion mechanism, especially for the smaller filament diameters investigated (i.e., with a contribution up to 75%), while electron impact dissociation contributes for about 20-40%, and electron impact dissociative attachment again contributes for up to 10% (at the larger filament diameters investigated).

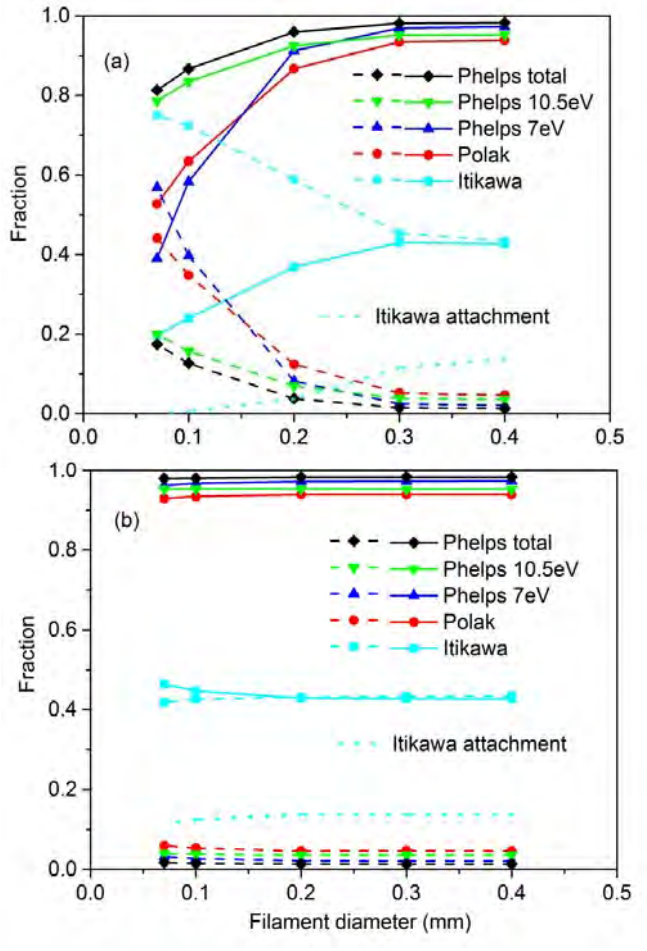

Figure 6: Relative contributions of the various dissociation mechanisms (i.e., electron impact dissociation, ionization and dissociative attachment) to the overall CO_2 conversion in the DBD plasma, calculated with the different dissociation cross sections, as a function of the assumed filament diameter, for $N_{e,max} = 10^{14}$ cm^{-3} (a), and the self-consistently calculated electron density, typically yielding $N_{e,max} \leq 10^{15}$ cm^{-3} (b), for a plasma power of 55 W (or an SEI of 4.2 eV/molec). The contributions of electron impact dissociation and ionization are indicated with solid and dashed lines, respectively. For the case of Itikawa's cross section, the contribution of electron impact dissociative attachment is also included (dotted line). For the other cross sections, the contribution of the latter process is negligible.

The reason why electron impact ionization becomes gradually more important as CO_2 conversion mechanism for the smallest filament diameters is again attributed to the higher reduced electric field and higher average electron energy (see Table 2), because the ionization rate coefficient rises more rapidly with higher reduced electric field and electron energy than the dissociation cross sections, as is obvious from Figure 3 above, due to its higher energy threshold. Moreover, Figure 3 also explains why electron impact ionization is more important for the CO_2 conversion than electron impact dissociation in case of Itikawa's cross section, certainly at $N_{e,max} = 10^{14}$ cm^{-3}, because its rate coefficient is higher, even for reduced electric fields around 100 Td, and thus for all filament diameters investigated, especially in case of $N_{e,max} = 10^{14}$ cm^{-3} (see Table 2). Likewise, it also explains why electron impact ionization is of comparable (or even higher) importance than electron impact dissociation for the Phelps 7 eV and Polak cross sections in case of the filament diameter of 0.07 mm, because the latter corresponds to a reduced electric field of 920 Td, at $N_{e,max} = 10^{14}$ cm^{-3} (see Table 2), and Figure 3 illustrates that for such high reduced electric field values, the ionization rate coefficient is higher than the dissociation rate coefficients calculated with the Phelps 7 eV and Polak cross sections.

The effect of the filament lifetime on the calculated CO_2 conversion is illustrated in Figure 7, for both $N_{e,max} = 10^{14}$ cm^{-3} (a) and $N_{e,max} = 10^{15}$ cm^{-3} (b), and for three different lifetimes and the five different cross sections, as indicated by the legends. The filament diameter is taken as 0.1 mm. The lifetime of 15.6 ns corresponds to the measured value of [36], but to assess the effect of this value, we also compare with a lifetime of 30 and 60 ns. In general, it is clear that the assumed value of the filament lifetime is not very critical. In some cases, the CO_2 conversion rises with rising lifetime, and in other cases it drops, but the difference is always limited to a few %, and smaller than the effect of the cross sections. Furthermore, we can conclude again from this figure that the CO_2 conversion calculated with all individual cross sections is lower than the measured value at this condition (i.e., 17.5 % [36]), except for the Phelps 10.5 eV cross section, which is comparable in case of $N_{e,max} = 10^{14}$ cm^{-3} (see Figure 7(a)), while the Phelps total cross section again overestimates the measured CO_2 conversion in all cases.

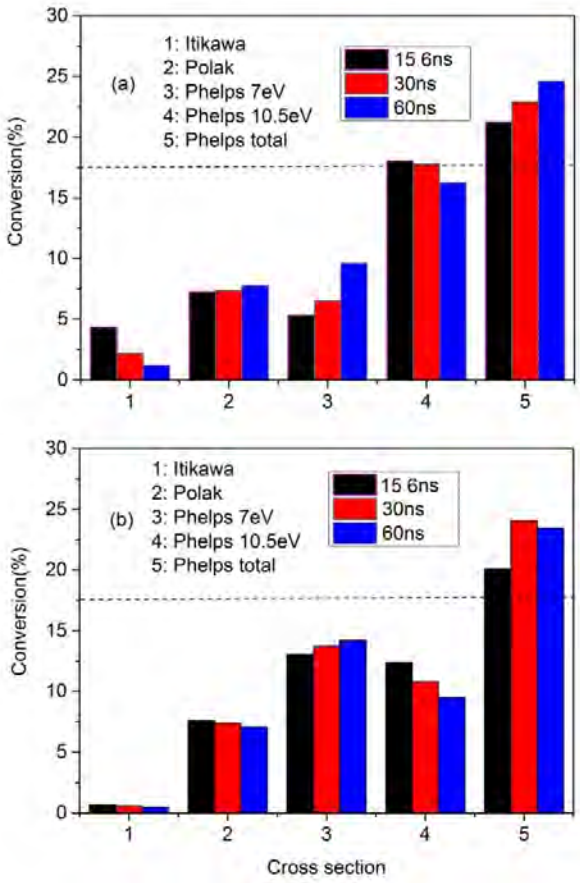

Figure 7: CO_2 conversion in the DBD plasma, calculated with the different dissociation cross sections and for different filament lifetimes, as indicated by the legends, for a filament diameter of 0.1 mm, and for $N_{e,max} = 10^{14}$ cm^{-3} (a), and the self-consistently calculated electron density, typically yielding $N_{e,max} \leq 10^{15}$ cm^{-3} (b), for a plasma power of 55 W (or an SEI of 4.2 eV/molec). For comparison, the measured value at this condition, obtained from [36], is indicated with the horizontal dashed line.

To evaluate which cross section yields a realistic CO_2 conversion in a wider range of plasma powers (or SEI values), we plot in Figure 8 the calculated CO_2 conversion, with the different cross sections, as a function of plasma power, and corresponding SEI value (for a gas flow rate of 200 mL/min), as well as the experimental values in the same range, as obtained from [36]. The results are obtained with the self-consistently calculated electron density, and for a filament lifetime of 15.6 ns, corresponding to the experimental value. The filament diameter is assumed to be 0.1 mm, as this is a typical value reported in literature [38-40], and Figure 5 indicated that this assumption is not so critical for the self-consistently calculated electron density. Possibly, the calculated CO_2 conversion with the different cross sections might be slightly overestimated when the actual filament diameter would be larger, but the difference will be at maximum only a few %.

As is obvious from Figure 8, Itikawa's cross section largely underestimates the CO_2 conversion in the entire range of SEI values, with values typically not larger than 1%. The same appears true, but to a lower extent, for Polak's cross section. The Phelps 7 eV and 10.5 eV cross sections yield comparable values for the CO_2 conversion in the entire range of SEI values, and they are also slightly lower than the measured values, while the sum of both Phelps cross sections overestimates the CO_2 conversion. The latter was also anticipated above, as these cross sections probably also include other excitation channels, not leading to

dissociation. From the comparison with the measured CO_2 conversion, and following also the recommendations of Pietanza et al. [28-30], we might conclude that the Phelps 7 eV cross section should give rise to dissociation, as well as a certain fraction (in the order of 30%) of the Phelps 10.5 eV cross section. However, because of the complexity of the entire plasma chemistry in our model, and the associated uncertainties of some of the assumptions made (in the rate coefficients as well as in the filament properties; see above), as well as possible uncertainties in the experimental data, it would be too dangerous to draw definite conclusions on which exact fraction of the Phelps 10.5 eV also contributes to dissociation.

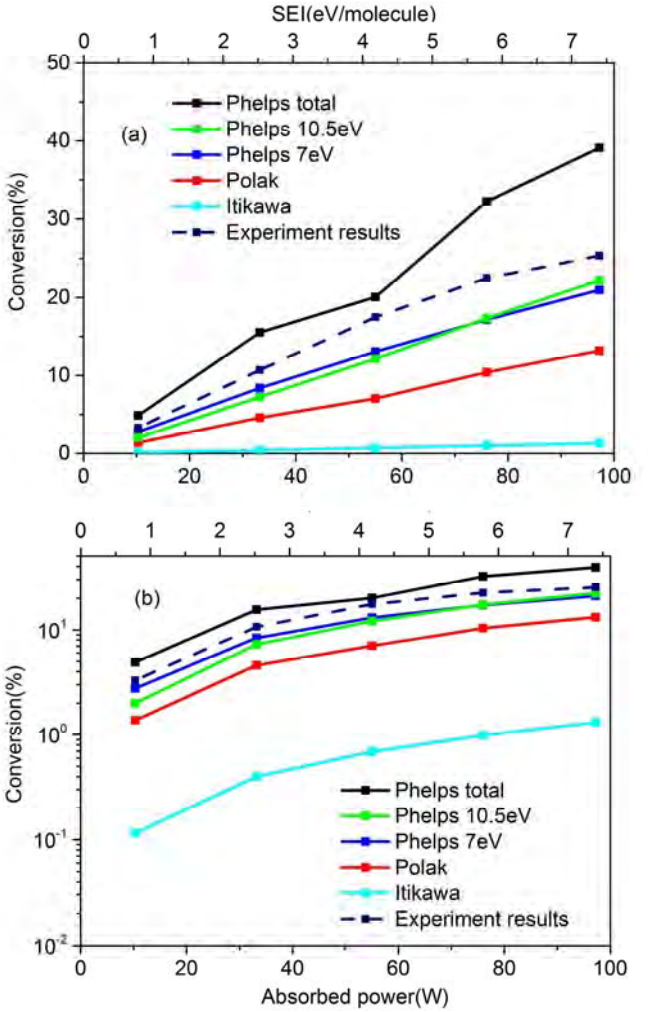

Figure 8: CO_2 conversion in the DBD plasma, calculated with the different dissociation cross sections, as a function of the plasma power and specific energy input (SEI), for a filament lifetime of 15.6 ns, a filament diameter of 0.1 mm, and the self-consistently calculated electron density, in linear y-scale (a) as well as logarithmic y-scale (b). For comparison, the measured values, obtained from [36], are included with the dashed line.

Our analysis suggests that future modeling studies may use the Phelps 7 eV cross section as representative of dissociation, although it should be kept in mind that it might neglect some additional dissociation channels (probably associated with the 10.5 eV threshold), and thus underestimate the actual CO_2

conversion. However, some uncertainty remains, as Ponduri et al. reported that applying the Phelps 7 eV cross section, in addition to Itikawa's cross section, already yielded a factor 2 overestimation compared to experimental values [15].

The rationale of taking into account two different cross sections with different energy thresholds, accounting for different excitation-dissociation channels to calculate the overall CO_2 conversion, is in correlation with the dissociation cross section reported by Fridman [11], which also contains two maxima, with a low and a high threshold energy. Moreover, our results are in line with the preliminary indications from [27], where the use of Polak's cross section was suggested as a good basis to analyse the question, and the direct comparison with Corvin's dissociation rate [34] shows that both Polak's and Phelps' 7 eV cross sections yield calculations in fairly good agreement with that earlier experiment, with slightly higher and better results for the 7 eV Phelps cross section.

It seems clear that there is a crucial need for further investigations on the CO_2 electron impact excitation-dissociation cross sections, from measurements or quantum chemical calculations, in order to elucidate which channels actually lead to effective dissociation.

3.2. MW plasma

Our previous model calculations [13,14] revealed that electron impact excitation-dissociation is not the dominant CO_2 conversion process in a MW plasma, because of the more important role of vibrational excitation, especially at high pressures. Therefore, a comparison of the CO_2 conversion in the MW plasma, calculated with the different dissociation cross sections, can probably not unambiguisly elucidate which cross section yields the most realistic CO_2 conversion. Nevertheless, it is still very interesting to evaluate the CO_2 conversion, as well as the relative importance of the various dissociation mechanisms at typical MW conditions, based on the different electron impact dissociation cross sections. Indeed, although our previous modeling study revealed that electron impact dissociation was of minor importance in a MW plasma, this study was performed with Itikawa's cross section, and it is clear now that the latter drastically underestimates the CO_2 conversion in a DBD, so it will probably also underestimate the importance of this process, and thus the overall CO_2 conversion in a MW plasma.

Figure 9 illustrates the CO_2 conversion, calculated with the five different cross sections, as a function of pressure in the MW plasma. All cross sections yield a maximum CO_2 conversion at a pressure of 200 mbar, which is similar to the values reported in literature [6,11]. Furthermore, again Itikawa's cross section yields the lowest CO_2 conversion, followed by the Polak and Phelps 10.5 eV cross sections, which yield more or less the same results. This is only coincidence, as their cross sections are clearly different. The Phelps 7 eV cross section yields a higher CO_2 conversion, while the value calculated with the total Phelps cross section is still somewhat higher.

The values obtained in Figure 9 appear to be realistic for typical MW conditions without supersonic or vortex flow. Unfortunately, we cannot directly compare these calculation results with experimental data, as there are not yet many data available for CO_2 conversion in a MW plasma in this wide pressure range, certainly not for a simple MW setup without supersonic or vortex flow. Indeed, it appears difficult to obtain a stable plasma using a simple laminar flow, without breaking the dielectric tube at higher pressures. Moreover, the few data available (e.g. [7,9]) are for somewhat different conditions (e.g., other SEI values or other tube radius and flow rate), or not all data necessary as input for the model are specified, thus not allowing a one-to-one comparison. Furthermore, by varying the gas temperature profile or the plasma length, we can match the experimental data with any of the cross section sets, so it would not be possible to draw conclusions from this. The purpose of this investigation is only to assess the effect of the

different cross sections on the calculated CO_2 conversion in the entire pressure range, and to provide information on the relative importance of the various dissociation mechanisms at these conditions.

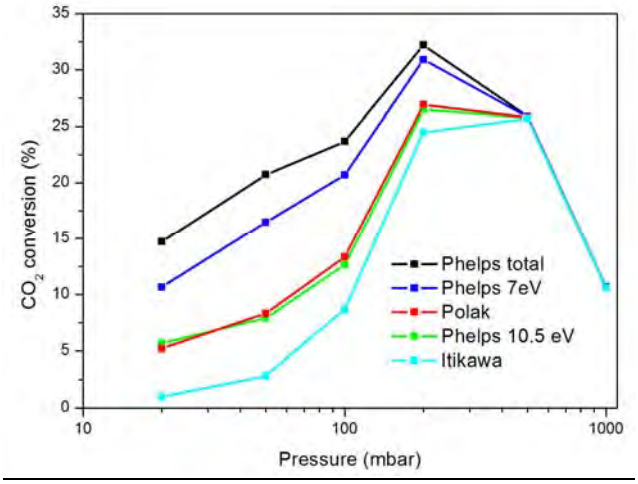

Figure 9: CO_2 conversion in the MW plasma, calculated with the different dissociation cross sections, as a function of pressure.

To evaluate which dissociation mechanism is the most important in the MW plasma in the pressure range investigated, and how this result is affected by the cross sections used, we plot the relative contributions of the four main dissociation mechanisms against pressure in Figure 10. The contributions of electron impact dissociation from the CO_2 ground state and from the vibrational levels are depicted in Figures 10(a) and 10(b), respectively. The sum of both processes appears to be the most important CO_2 conversion mechanism at very low pressures, for all cross sections investigated, except for Itikawa's cross section. This shows indeed that our previous calculations underestimated the relative contribution of this process, and that the choice of the dissociation cross section is also important in a MW plasma, at least at low pressure. At 20 mbar, electron impact dissociation is clearly dominant, with a calculated contribution of 70-80%, for all cross sections (except Itikawa), but this value drops significantly towards higher pressures. At 50 mbar, it contributes for about 50%, while at 100 mbar, it contributes for about 20-35%, and at still higher pressures it becomes negligible. The reason why its contribution drops upon higher pressure is because of the lower ionization degree at higher pressure, and thus, electron impact reactions in general become less important. By comparing Figures 10(a) and 10(b), it is clear that electron impact dissociation from the CO_2 vibrational levels is more important than dissociation from the ground state, with a relative contribution that is typically 3 times higher, thus accounting for about 75% of the overall process of electron impact excitation-dissociation. This indicates the important role of the vibrational levels for CO_2 conversion in a MW plasma.

The drop in the relative contribution of electron impact dissociation upon increasing pressure is accompanied by a significant rise in the contribution of dissociation through O atom impact with CO_2 (being either in the ground state or in vibrationally excited levels), i.e., $CO_2 + O \rightarrow CO + O_2$, for all cross sections investigated (see Figure 10(c)). Indeed, while this process only contributes for about 15-20% at 20 mbar, for all cross sections investigated, its relative importance rises significantly with pressure, reaching values above 50% at 100 mbar, and even above 90% for pressures of 500 mbar and higher. The reason why this process becomes more important at higher pressure is simply because of the higher O atom density.

Finally, as is clear from Figure 10(d), the dissociation of CO_2 upon collision with other heavy particles, i.e., $CO_2 + M \rightarrow CO + O + M$, with M being any type of molecule and CO_2 being either in the ground state or in a vibrational level, has a contribution of about 5-20%, in the entire pressure range investigated, being somewhat higher at 100 mbar for all cross sections investigated, except for Itikawa's cross section, where its contribution is calculated to be 50% at the lowest pressures investigated. The latter is of course attributed to the smaller contribution of electron impact dissocation with this cross section, as illustrated in Figure 10(a). One would expect this process to become more important upon higher pressure; the reason that this is not apparent from Figure 10(d) is because of the increasing role of dissociation upon collision with O atoms (Figure 10(c)). However, it is clear that if we consider the sum of both processes due to heavy particle collisions, their total contribution rises with pressure.

In general, we can conclude for the MW plasma that the effect of using different cross sections for electron impact excitation is somewhat smaller than for the DBD, especially at the higher pressures, which are mainly of interest for this application. Nevertheless, at low pressure, the effect is still considerable, and this is due to the non-negligible contribution of electron impact dissociation to the overall CO_2 conversion in this lower pressure range. At high pressure, however, the collision of O atoms with CO_2 (being either in the ground state or in vibrationally excited levels) is the dominant dissociation mechanism in the MW plasma.

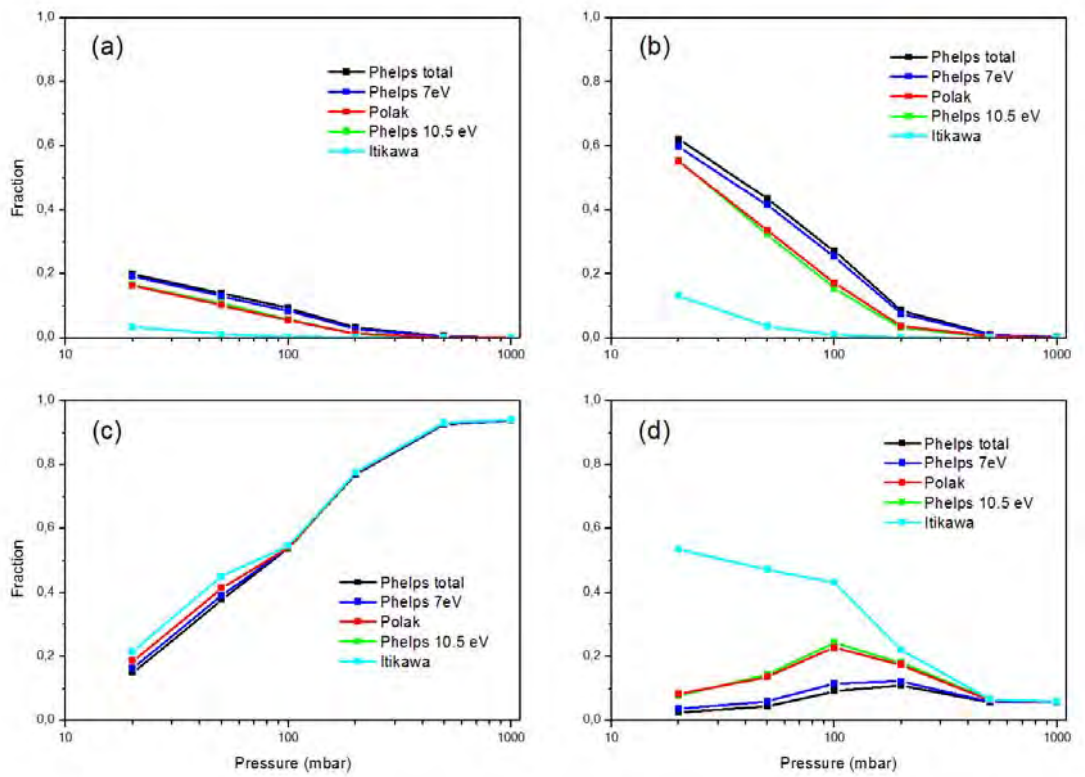

Figure 10: Relative contributions of the main dissociation processes leading to CO_2 conversion in the MW plasma, calculated with the different dissociation cross sections, as a function of pressure: (a) electron impact excitation-dissociation from the CO_2 ground state, (b) electron impact excitation-dissociation from the CO_2 vibrational levels, (c) dissociation upon impact of O atoms, (d) dissociation upon collision with other heavy particles.

4. Conclusion

We performed a detailed study on the effect of different CO_2 dissociation cross sections on the CO_2 conversion in a range of different plasma conditions, for a DBD and MW plasma reactor. Indeed, there is quite some uncertainty in literature on which cross section captures the correct mechanisms of electron impact dissociation, with possible contributions from different excitation channels.

More specifically, we compared the results for the cross section reported by Itikawa, with a threshold energy of 11.9 eV, the cross sections reported by Phelps, with threshold energies of 7 eV and 10.5 eV, as well as the sum of both cross sections, thus representing two different excitation channels leading to dissociation, and the total cross section calculated by Polak and Slovetsky, also consisting of two different excitation-dissociation channels.

Our calculations reveal that the choice of the dissociation cross section is critical to obtain an accurate conversion in a DBD, where electron impact dissociation is the dominant mechanism for CO_2 conversion. The relative importance of the main dissociation mechanisms, as calculated by the model, depends on the cross section used, as well as on the filament conditions assumed in the model. We have investigated the effect of the (maximum) electron density in the DBD filaments, as well as of using different filament diameters and lifetimes, for the different cross sections, to make sure that our conclusions on the most realistic cross section do not depend on the filament assumptions. By comparing our calculated CO_2 conversion as a function of plasma power, or SEI values, with measured values for the same operating conditions, we can conclude that the cross sections proposed by Itikawa and by Polak and Slovetsky both underestimate the CO_2 conversion. The difference is most pronounced for the Itikawa cross section, which yields CO_2 conversions not higher than 1% in the entire range of SEI values. The cross sections reported by Phelps with threshold of 7 eV and 10.5 eV yield a CO_2 conversion only slightly lower than the experimental data, but the sum of both cross sections overestimates the values. This indicates that these cross sections most probably also include other excitation channels, not leading to dissociation.

Because of the complexity of the plasma chemistry in our model, and the uncertainties of some of the assumptions made, as well as possible uncertainties in the experimental data, it is a bit premature to draw definite conclusions on which cross section yields the most realistic CO_2 conversion. However, we believe that the Phelps cross section with 7 eV threshold should give rise to dissociation, as well as a certain fraction of the Phelps cross section with 10.5 eV threshold. It would be interesting if in the future an explanation can be given, based on the atomic physics picture of the collision process, why the 7 eV and (part of the) 10.5 eV threshold cross sections of Phelps might also lead to a CO_2 dissociation channel, but this is outside the scope of the present paper.

The rationale of accounting for two different cross sections with different energy thresholds, representing different excitation-dissociation channels to calculate the overall CO_2 conversion, is in correlation with the dissociation cross section reported by Fridman [11] and with the conclusions drawn by Grofulović et al. [27] that Polak's cross section might provide a good theoretical basis, as they are both also based on two different excitation channels, corresponding to a lower and a higher threshold energy.

In the MW plasma, the effect of the different electron impact dissociation cross sections is smaller, and greatly depends on the gas pressure. Indeed, at pressures above 100 mbar, dissociation typically proceeds by collisions of heavy particles with CO_2, and thus the choice of the electron impact dissociation cross section is less crucial. However, at pressures up to 100 mbar, electron impact dissociation still appears to be the major dissocation pathway, and thus the CO_2 conversion calculated with the different cross sections is quite different.

In general, our calculations indicate that especially for the DBD plasma more detailed investigations on the CO_2 electron impact excitation-dissociation cross sections, either through measurements or quantum

chemical calculations, are crucially needed to elucidate which excitation channels actually lead to dissociation. As long as this is not known, we consider that future modeling studies may use the Phelps 7 eV cross section, keeping in mind that it might neglect some additional dissociation channels (probably associated with the 10.5 eV threshold), and thus it might underestimate to some extent the actual CO_2 conversion. However, further work is necessary to completely clarify this issue.

Acknowledgements

The authors would like to thank R. Snoeckx and S. Heijkers for the interesting discussions. This research was supported by the European Union's Seventh Framework Programme for research, technological development and demonstration under grant agreement no. 606889, the European Marie Skłodowska-Curie Individual Fellowship project "GlidArc" within Horizon2020, the FWO project (grant G.0383.16N), and the Network on Physical Chemistry of Plasma-Surface Interactions - Interuniversity Attraction Poles, phase VII (PSI-IAP7), supported by the Belgian Science Policy Office (BELSPO). The computational work was carried out using the Turing HPC infrastructure at the CalcUA core facility of the Universiteit Antwerpen (UA), a division of the Flemish Supercomputer Center VSC, funded by the Hercules Foundation, the Flemish Government (department EWI) and the UA. VG was partially supported by the Portuguese FCT – Fundação para a Ciência e a Tecnologia, under Project UID/FIS/50010/2013.

References

1. Zhang J, Zhu A M, Guo J, Xu Y and Shi C 2010 *Chem. Eng. J.* **156** 601
2. Aerts R, Somers W and Bogaerts A 2015 *ChemSusChem.* **8**, 702
3. Yu Q, Kong M, Liu T, Fei J and Zheng X 2012 *Plasma Chem. Plasma Process.* **32** 153
4. Mei D, Zhu X, He Y, Yan Y D and Tu X 2015 *Plasma Sources Sci. Technol.* **24** 015011
5. Van Laer K and Bogaerts A 2015 *Energy Technol.* **3** 1038–1044
6. Asisov R I, Givotov V K, Krasheninnikov E G, Potapkin B V, Rusanov V D and Fridman A 1983 *Sov. Phys., Doklady* **271** 94
7. Silva T, Britun N, Godfroid T and Snyders R 2014 *Plasma Sources Sci. Technol*. **23** 025009
8. Goede A P H, Bongers W A, Graswinckel M G, van de Sanden M C M, Martina L, Jochen K, Schulz A and Mathias W 2014 *EPJ Web of Conferences*, 3rd Eur. Energy Conference, Budapest 2014, 01005, 1–5
9. Spencer L F and Gallimore A D 2013 *Plasma Sources Sci. Technol.* **22** 015019
10. Bongers W A, Welzel S, van den Bekerom D C M, Frissen G, van Rooij G J, Goede A P H, Graswinckel M F, Groen P, den Harder N, van Heemert B, et al., Proceedings 22nd International Symposium on Plasma Chemistry (Antwerp, Belgium), 2015
11. Fridman A 2008 Plasma Chemistry (Cambridge University Press, Cambridge)
12. Aerts R, Martens T and Bogaerts A 2012 *J. Phys. Chem. C* **116** 23257
13. Kozák T and Bogaerts A 2014 *Plasma Sources Sci. Technol.* **23** 045004
14. Kozák T and Bogaerts A 2015 *Plasma Sources Sci. Technol.* **24** 015024
15. Ponduri S, Becker M M, Welzel S, van de Sanden M C M, Loffhagen D and Engeln R 2016 *J. Appl. Phys*. **119** 093301
16. Berthelot A and Bogaerts A 2016 *Plasma Sources Sci. Technol.* **25** 045022
17. Snoeckx R, Aerts R, Tu X and Bogaerts A 2013 *J. Phys. Chem. C* **117** 4957
18. Snoeckx, Zeng Y X, Tu X and Bogaerts A 2015 *RSC Advances* **5** 29799
19. Snoeckx R, Heijkers S, Van Wesenbeeck K, Lenaerts S and Bogaerts A 2016 *Energy & Environm. Sci.* **9** 999-1011

20. Heijkers S, Snoeckx R, Kozák T, Silva T, Godfroid T, Britun N, Snyders R and Bogaerts A 2015 *J. Phys. Chem. C* **119** 12815-12828
21. Janeco A, Pinhão N R and Guerra V 2015 *J. Phys. Chem. C* **119** 109
22. Bogaerts A, Kozák T, Van Laer K and Snoeckx R 2015 *Faraday Discussions* **183** 217-232
23. Phelps Database, www.lxcat.net, retrieved on December 1, 2015
24. Lowke J J, Phelps A V and Irwin B W 1973 *J. Appl. Phys*. **44** 4664-4671
25. Hake R D Jr., Phelps A V 1967 *Phys. Rev.* **158** 70-84
26. Itikawa Database, www.lxcat.net, retrieved on December 1, 2015. Itikawa Y 2002 *J. Phys. Chem*. **R31** 749-767
27. Grofulović M, Guerra V, Alves L L, *J. Phys. D: Appl. Phys* (submitted)
28. Pietanza L D, Colonna G, D'Ammando G, Laricchiuta A and Capitelli M 2015 *Plasma Sources Sci. Technol*. **24** 042002
29. Pietanza L D, Colonna G, D'Ammando G, Laricchiuta A and Capitelli M 2016 *Phys. Plasmas* **23** 013515
30. Pietanza L D, Colonna G, D'Ammando G, Laricchiuta A and Capitelli 2016 *Chem. Phys.* **468** 44
31. Pietanza L D, Colonna G, Laporta V, Celiberto R, D'Ammando G, Laricchiuta A and Capitelli M 2016 *J. Phys. Chem. A* **120** 2614
32. Cosby P C, Helm H 1993 "Dissociation rates of diatomic molecules", Report, AD-A266 464, WL-TR-93-2004
33. Polak L S, Slovetsky D I 1976 *Int. J. Radiat. Phys. Chem*. **8** 257-282
34. Corvin K K and Corrigan S J B 1969 *J. Chem. Phys*. **50** 2570-2574
35. Pancheshnyi S, Eismann B, Hagelaar G J M and Pitchford L C, Computer code ZDPlasKin, http://www.zdplaskin.laplace.univ-tlse.fr (University of Toulouse, LAPLACE, CNRS-UPS-INP, Toulouse, France, 2008).
36. Ozkan A, Dufour T, Silva T, Snyders R, Bogaerts A and Reniers R 2016 *Plasma Sources Sci. Technol.* **25**, 025013
37. Samoilovich V G, Gibalov V I and Kozlov K V 1997 *Physical Chemistry of the Barrier Discharge* 2nd ed. (Düsseldorf: Deutscher Verlag für Schweisstechnik)
38. Fridman A, Chirokov A and Gutsol A 2005 *J. Phys. D: Appl. Phys*. **38** R1–R24
39. Kogelschatz U 2002 *IEEE Trans Plasma Sci* **30** 1400 – 1408